Available online at www.sciencedirect.com
SCIENCE DIRECT®
Journal of Magnetic Resonance 163 (2003) 199–207
JMR Journal of Magnetic Resonance
www.elsevier.com/locate/jmr

Transferred cross-relaxation and cross-correlation in NMR: effects of intermediate exchange on the determination of the conformation of bound ligands

Sapna Ravindranathan,[a] Jean-Maurice Mallet,[b] Pierre Sinay,[b] and Geoffrey Bodenhausen[a,b,*]

[a] *Institut de Chimie Moléculaire et Biologique, Ecole Polytechnique Fédérale de Lausanne, BCH, 1015 Lausanne, Switzerland*
[b] *Département de Chimie, associé au CNRS, Ecole Normale Supérieure, 24, Rue Lhomond, 75231 Paris Cedex 05, France*

Received 16 December 2002; revised 28 March 2003

Abstract

Exchange transferred effects in solution-state NMR experiments allow one to determine the conformation of ligands that are weakly bound to macromolecules. Exchange-transferred nuclear Overhauser effect spectroscopy ('TR-NOESY') provides information about internuclear distances in a ligand in the bound state. Recently the possibility of obtaining dihedral angle information from a ligand in the bound state by exchange-transferred cross-correlation spectroscopy ('TR-CCSY') has been reported. In both cases the analysis of the signal amplitudes is usually based on the assumption that rapid exchange occurs between the free and bound forms of the ligand. In this paper we show that the fast exchange condition is not easily attained for observing exchange-transferred cross-correlation effects even in systems where exchange-transferred NOE can be observed. Extensive simulations based on analytical expressions for signal intensities corresponding to fast, intermediate, and slow chemical exchange have been carried out on a test system to determine the exchange regimes in which the fast exchange condition can be fulfilled for successfully implementing TR-NOESY and TR-CCSY.

1. Introduction

The conformation of cofactors, inhibitors, and other ligands that are bound to macromolecules is of considerable interest for pharmaceutical chemistry. Exchange transferred nuclear Overhauser spectroscopy (TR-NOESY) allows one to determine internuclear distances in the bound state through cross-relaxation [1,2]. The cross-relaxation process, which is rapid in the slowly tumbling complex ML, results in a partial interconversion of angular momentum operators representing populations (e.g., I_{kz} to I_{lz}) associated with the bound ligand. The resulting populations are partly preserved (on the time scale of the longitudinal relaxation time T_1) when the complex ML dissociates into free ligand L and free macromolecule M. One can thus effectively observe Overhauser effects on the narrow resonances of the free ligand that reflect the conformation in the bound state. Recently it has been shown [3,4] that similar principles are applicable to transferred cross-correlation spectroscopy, which we shall refer to as TR-CCSY. In this case a two-spin coherence such as $2C_{kx}C_{lx}$ associated with the ligand may be partially converted to an antiphase term such as $8C_{ky}H_{kz}C_{ly}H_{lz}$ through cross-correlated dipolar interactions while the ligand is in the bound state. Alternatively, one may monitor the interconversion of $4C_{kx}H_{kz}C_{lx}$ into $4C_{ky}C_{ly}H_{lz}$ under the same dipolar interactions. The rate of such an interconversion, which is proportional to the correlation time τ_c of the complex ML, provides direct evidence of angles subtended between various spin interactions, which in turn can be related to dihedral angles. The resulting coherences are partly preserved, albeit on the time scale of the transverse relaxation time T_2 of the coherences, when the complex dissociates into free ligand and free

* Corresponding author. Fax: +33-1-44-32-33-97.
E-mail address: geoffrey.bodenhausen@ens.fr (G. Bodenhausen).

1090-7807/$ - see front matter © 2003 Elsevier Science (USA). All rights reserved.
doi:10.1016/S1090-7807(03)00156-3

macromolecule. By observing narrow resonances of the free ligand it is therefore possible to monitor cross-correlation effects that reveal information about the conformation of the ligand in the bound state ML. In this paper, analogies and differences between TR-NOESY and TR-CCSY are discussed in some detail.

Cross-correlation effects have proven to be a valuable source of structural and dynamic information in macromolecules [5,6]. Cross-correlation effects between different spin interactions have been exploited to obtain dihedral angles in proteins and sugar moieties in nucleic acids [7–12]. The general strategy for determining dihedral angles from a quantitative measurement of cross-correlated relaxation rates involves identifying a three- or four-spin system spanning the angle of interest and exciting suitable multiple quantum coherences. During a period τ_m, this coherence will not merely decay (self-relaxation) but it may be partly converted into other coherences (cross-correlated relaxation) under various interference terms involving fluctuating spin Hamiltonians. This interconversion can be monitored by suitably designed experimental sequences. The influence of different interference terms is most readily visualized in a cartesian product operator representation of the coherences. This amounts to examining the relaxation behaviour of the sums or differences of multiplet components in multiple quantum spectra. In the following section we examine this in more detail.

2. Relaxation mediated coherence or magnetisation transfer

The coherences evolve under the spin Hamiltonian which is comprised of a sum of isotropic terms (chemical shifts and J-couplings) and randomly modulated anisotropic parts. The experiments for measuring cross-correlation rates which we consider in this paper are designed so that the evolution under the isotropic part of the spin Hamiltonian during the relaxation period τ_m is refocussed [7,11]. We therefore restrict the following discussion to the effects of the anisotropic parts of the Hamiltonian on the coherences. The relaxation of the coherences under a randomly modulated Hamiltonian can be described by

$$\frac{d\boldsymbol{v}}{dt} = -\boldsymbol{\Gamma}\boldsymbol{v}. \tag{1}$$

Here, $\boldsymbol{v}$ represents the n-dimensional vector of the expectation values of the multiple quantum coherences and $\boldsymbol{\Gamma}$ is the $n \times n$ relaxation matrix. The diagonal elements of $\boldsymbol{\Gamma}$ correspond to sums of auto-correlation terms whereas the non-zero off-diagonal elements involve cross-correlated relaxation rates. The off-diagonal elements thus provide relaxation pathways which lead to coherence transfer. The elements of $\boldsymbol{v}$ may also represent expectation values of angular momentum operators such as I_{kz} and I_{lz} corresponding to populations. In this case, Eq. (1) describes the time evolution of longitudinal magnetisation modes [5]. The experimental approach for determining a given cross-relaxation rate involves isolating a specific off-diagonal element from the $n \times n$ matrix. This can often be achieved by inserting suitably positioned π pulses in the relaxation interval [6–8,13]. In favourable cases, the $n \times n$ matrix can thus be reduced to a 2×2 relaxation matrix and the vector $\boldsymbol{v}$ has the form

$$\begin{bmatrix} v_1 \\ v_2 \end{bmatrix},$$

while the matrix $\boldsymbol{\Gamma}$ is of the form

$$\begin{bmatrix} \Gamma_{1a} & \Gamma_c \\ \Gamma_c & \Gamma_{2a} \end{bmatrix}.$$

Coherence transfer is brought about by the cross-relaxation rate denoted Γ_c while Γ_{1a} and Γ_{2a} are the self-relaxation rates (sums of auto-correlation terms) of the two coherences. For example, the coherence transfer S_x to $2S_xI_z$ may result from cross-correlation between the chemical shift anisotropy of S and the dipolar coupling between S and I. When isolated spin systems are considered, $\Gamma_{1a} = \Gamma_{2a} = \Gamma_a$ is often a reasonable approximation. Coherence transfer is analogous to longitudinal magnetisation transfer (e.g., I_{kz} to I_{lz}) mediated by cross-relaxation in a NOESY experiment.

Usually two experiments must be performed, a reference experiment (I) which allows one to detect the expectation value v_1 of the initial coherence and a complementary experiment (II) designed to detect the expectation value v_2 of the coherence resulting from a transfer brought about by cross-correlated relaxation [7]. The amplitudes of the signals observed in the two experiments are given by

$$a_I \propto \cosh(\Gamma_c\tau_m)\exp(-\Gamma_a\tau_m), \tag{2}$$

$$a_{II} \propto \sinh(\Gamma_c\tau_m)\exp(-\Gamma_a\tau_m), \tag{3}$$

where τ_m is the relaxation period. The cross-correlated relaxation rate Γ_c can be readily obtained from the ratio of the amplitudes of the signals measured in experiments II and I.

$$\frac{a_{II}}{a_I} = \tanh(\Gamma_c\tau_m). \tag{4}$$

This is in contrast to the NOESY experiment in which both terms v_1 and v_2 are detected in a single experiment in the form of diagonal and cross-peaks. Also, in NOESY the assumption that $\Gamma_{1a} = \Gamma_{2a} = \Gamma_a$ can usually only be fulfilled for an isolated two-spin system, whereas this assumption is often more realistic in CCSY.

Recently, cross-correlation spectroscopy (CCSY) has been applied to systems in chemical exchange to deter-

mine dihedral angles in a ligand which is weakly bound to a macromolecule [3,4]. This type of experiment which, we shall refer to as TR-CCSY, is analogous to the well known TR-NOESY experiments which provide internuclear distance information in ligands bound to macromolecules [2]. We examine here the conditions that must be fulfilled for exchange transferred cross-correlated relaxation rate measurements for studying the conformation of bound ligands.

3. Exchange transferred cross-correlated relaxation

The exchange equilibrium involving a ligand (L) and a macromolecule (M) can be represented as

$$\mathrm{M} + \mathrm{L} \underset{k_{-1}}{\overset{k_1}{\rightleftharpoons}} \mathrm{ML}$$

The dissociation constant for the reaction is given by

$$K_\mathrm{d} = \frac{k_{-1}}{k_1} = \frac{[\mathrm{L}][\mathrm{M}]}{[\mathrm{ML}]}, \tag{5}$$

where [L], [M], and [ML] are the concentrations of the free ligand, free macromolecule, and the complex, respectively. The equilibrium may also be expressed in terms of the concentrations of the free and bound forms of the ligand by defining a pseudo-first order forward rate constant $k_\mathrm{on} = k_1[\mathrm{M}]$, and by calling the rate constant for the backward reaction $k_\mathrm{off} = k_{-1}$.

$$\frac{k_\mathrm{on}}{k_\mathrm{off}} = \frac{[\mathrm{ML}]}{[\mathrm{L}]} = \frac{p_\mathrm{ML}}{p_\mathrm{L}} = F. \tag{6}$$

Here, the fraction of bound ligand is $p_\mathrm{ML} = [\mathrm{ML}]/([\mathrm{ML}] + [\mathrm{L}])$ and the fraction of the free ligand is $p_\mathrm{L} = [\mathrm{L}]/([\mathrm{ML}] + [\mathrm{L}])$. Typically F is of the order of 0.1 or less since the experiments are carried out in the presence of a large excess of free ligand.

For exchanging systems, the vector $\boldsymbol{v}$ in Eq. (1) must be extended to encompass the expectation values of the coherences in the complex ML and in the free form L, and the matrix $\boldsymbol{\Gamma}$ must incorporate both relaxation and chemical exchange rates. The vector $\boldsymbol{v}$ now takes the form

$$\begin{bmatrix} v_1^\mathrm{ML} \\ v_2^\mathrm{ML} \\ v_1^\mathrm{L} \\ v_2^\mathrm{L} \end{bmatrix}$$

and the extended relaxation matrix $\boldsymbol{\Gamma}$ is given by

$$\begin{bmatrix} \Gamma_\mathrm{a}^\mathrm{ML} + k_\mathrm{off} & \Gamma_\mathrm{c}^\mathrm{ML} & -k_\mathrm{off}F & 0 \\ \Gamma_\mathrm{c}^\mathrm{ML} & \Gamma_\mathrm{a}^\mathrm{ML} + k_\mathrm{off} & 0 & -k_\mathrm{off}F \\ -k_\mathrm{off} & 0 & \Gamma_\mathrm{a}^\mathrm{L} + k_\mathrm{off}F & \Gamma_\mathrm{c}^\mathrm{L} \\ 0 & -k_\mathrm{off} & \Gamma_\mathrm{c}^\mathrm{L} & \Gamma_\mathrm{a}^\mathrm{L} + k_\mathrm{off}F \end{bmatrix},$$

where k_on has been replaced by $k_\mathrm{off}F$.

The relaxation rates with superscripts ML and L refer to the bound and free states, respectively. The solution of the differential equation is obtained by diagonalizing the matrix $\boldsymbol{\Gamma}$, so that the time dependence of the elements of $\boldsymbol{v}$ can be expressed as linear combinations of exponentials of the eigenvalues of $\boldsymbol{\Gamma}$. In the limiting case of $k_\mathrm{off} = 0$, the free and bound states clearly form two isolated systems and there is no transfer of any information from the bound state to the free state. The signal amplitudes of experiments I and II are then described by the pair of Eqs. (2) and (3) separately for the bound and free states. As k_off increases there is a mixing of the elements of $\boldsymbol{\Gamma}$ which results in a transfer of information about relaxation from the bound state to the free state. The evolution of coherences during the relaxation interval τ_m is described by

$$\boldsymbol{v}(\tau_\mathrm{m}) = \boldsymbol{S}(\tau_\mathrm{m})\boldsymbol{v}(0), \tag{7}$$

where $\boldsymbol{S}(\tau_\mathrm{m}) = \boldsymbol{X}\exp(-\boldsymbol{D}\tau_\mathrm{m})\boldsymbol{X}^{-1}$, $\boldsymbol{X}$ is the matrix of eigenvectors of $\boldsymbol{\Gamma}$ and $\boldsymbol{D}$ is a diagonal matrix containing the eigenvalues of $\boldsymbol{\Gamma}$. In the case of TR-NOESY, the vector $\boldsymbol{v}$ contains the expectation values of the longitudinal magnetisation components $\langle I_{kz}\rangle^\mathrm{ML}$, $\langle I_{lz}\rangle^\mathrm{ML}$, $\langle I_{kz}\rangle^\mathrm{L}$, and $\langle I_{lz}\rangle^\mathrm{L}$ corresponding to the spins in the bound and free states. In the case of TR-CCSY, the vector $\boldsymbol{v}$ contains expectation values such as $\langle 4\mathrm{C}_{kx}\mathrm{H}_{kz}\mathrm{C}_{lx}\rangle^\mathrm{ML}$, $\langle 4\mathrm{C}_{ky}\mathrm{C}_{ly}\mathrm{H}_{lz}\rangle^\mathrm{ML}$, $\langle 4\mathrm{C}_{kx}\mathrm{H}_{kz}\mathrm{C}_{lx}\rangle^\mathrm{L}$, and $\langle 4\mathrm{C}_{ky}\mathrm{C}_{ly}\mathrm{H}_{lz}\rangle^\mathrm{L}$. In general, the self-relaxation rates cannot be assumed to be equal although this assumption may be easier to fulfill in CCSY than in NOESY. The time evolution of the magnetisation can be obtained numerically after a suitable transformation to make the matrix symmetric [14–16]. In TR-CCSY however, the experimental scheme allows the dimensionality of the problem to be reduced, and the self-relaxation rates of the coherences can often be assumed to be equal. The analytical solution for the time evolution of the magnetisation in a chemically exchanging system has been derived in the context of TR-NOESY for a two spin system [17]. Here, we recast the general solutions in a format that readily allows us to express the signal amplitudes measured in experiments I and II as a function of k_off. These expressions then allow us to simulate signal intensities (a_I and a_II) in TR-CCSY over all exchange regimes. The eigenvalues of $\boldsymbol{\Gamma}$ obtained by solving the characteristic equation are given by

$$D_1 = \frac{1}{2}\left[(\Gamma_\mathrm{a}^\mathrm{ML} + \Gamma_\mathrm{c}^\mathrm{ML}) + (\Gamma_\mathrm{a}^\mathrm{L} + \Gamma_\mathrm{c}^\mathrm{L}) + k_\mathrm{off}(1+F) + \Delta_1\right], \tag{8}$$

$$D_2 = \frac{1}{2}\left[(\Gamma_\mathrm{a}^\mathrm{ML} + \Gamma_\mathrm{c}^\mathrm{ML}) + (\Gamma_\mathrm{a}^\mathrm{L} + \Gamma_\mathrm{c}^\mathrm{L}) + k_\mathrm{off}(1+F) - \Delta_1\right], \tag{9}$$

$$D_3 = \frac{1}{2}\left[(\Gamma_\mathrm{a}^\mathrm{ML} - \Gamma_\mathrm{c}^\mathrm{ML}) + (\Gamma_\mathrm{a}^\mathrm{L} - \Gamma_\mathrm{c}^\mathrm{L}) + k_\mathrm{off}(1+F) + \Delta_2\right], \tag{10}$$

$$D_4 = \frac{1}{2}\left[(\Gamma_a^{ML} - \Gamma_c^{ML}) + (\Gamma_a^{L} - \Gamma_c^{L}) + k_{off}(1+F) - \Delta_2\right]. \tag{11}$$

The factors Δ_1 and Δ_2 are given by

$$\Delta_1 = \{[(\Gamma_a^{ML} + \Gamma_c^{ML}) - (\Gamma_a^{L} + \Gamma_c^{L})]^2 + 2k_{off}(1-F) \times [(\Gamma_a^{ML} + \Gamma_c^{ML}) - (\Gamma_a^{L} + \Gamma_c^{L})] + k_{off}^2(1+F)^2\}^{1/2}, \tag{12}$$

$$\Delta_2 = \{[(\Gamma_a^{ML} - \Gamma_c^{ML}) - (\Gamma_a^{L} - \Gamma_c^{L})]^2 + 2k_{off}(1-F) \times [(\Gamma_a^{ML} - \Gamma_c^{ML}) - (\Gamma_a^{L} - \Gamma_c^{L})] + k_{off}^2(1+F)^2\}^{1/2}. \tag{13}$$

The signal amplitudes measured in experiments I and II are proportional to the elements S_{33} and S_{43} of the matrix $\boldsymbol{S}$. The elements S_{kl} are of the form

$$S_{kl} = \sum_{i=1}^{4} c_{kl,i} \exp(-D_i \tau_m), \tag{14}$$

where D_i are the eigenvalues of $\boldsymbol{\Gamma}$ and $c_{kl,i}$ are coefficients. The coefficients for the element S_{43} which determine the signal amplitudes in experiment II are given by

$$c_{43,1} = -\frac{1}{4}\left\{\frac{[(\Gamma_a^{ML} + \Gamma_c^{ML}) - (\Gamma_a^{L} + \Gamma_c^{L}) + k_{off}(1-F)]}{\Delta_1} - 1\right\}, \tag{15}$$

$$c_{43,2} = \frac{1}{4}\left\{\frac{[(\Gamma_a^{ML} + \Gamma_c^{ML}) - (\Gamma_a^{L} + \Gamma_c^{L}) + k_{off}(1-F)]}{\Delta_1} + 1\right\}, \tag{16}$$

$$c_{43,3} = \frac{1}{4}\left\{\frac{[(\Gamma_a^{ML} - \Gamma_c^{ML}) - (\Gamma_a^{L} - \Gamma_c^{L}) + k_{off}(1-F)]}{\Delta_2} - 1\right\}, \tag{17}$$

$$c_{43,4} = -\frac{1}{4}\left\{\frac{[(\Gamma_a^{ML} - \Gamma_c^{ML}) - (\Gamma_a^{L} - \Gamma_c^{L}) + k_{off}(1-F)]}{\Delta_2} + 1\right\}. \tag{18}$$

Similar coefficients determine the signal amplitudes S_{33} of experiment I except for some of the signs: $c_{33,1} = c_{43,1}$, $c_{33,2} = c_{43,2}$, $c_{33,3} = -c_{43,3}$, and $c_{33,4} = -c_{43,4}$.

We now examine the signal amplitudes in experiments I and II for the limit of large k_{off}. The factors Δ_1 and Δ_2 have the form

$$\Delta_{1,2} = k_{off}(1+F)\left[1 + \frac{2(1-F)x}{(1+F)^2 k_{off}} + \frac{x^2}{(1+F)^2 k_{off}^2}\right]^{1/2}, \tag{19}$$

where $x = (\Gamma_a^{ML} + \Gamma_c^{ML}) - (\Gamma_a^{L} + \Gamma_c^{L})$ for Δ_1 and $x = (\Gamma_a^{ML} - \Gamma_c^{ML}) - (\Gamma_a^{L} - \Gamma_c^{L})$ for Δ_2. Expanding in a series at $k_{off}^{-1} = 0$ gives the following eigenvalues:

$$D_1 = k_{off}(1+F) + p_L(\Gamma_a^{ML} + \Gamma_c^{ML}) + p_{ML}(\Gamma_a^{L} + \Gamma_c^{L}), \tag{20}$$

$$D_2 = p_{ML}(\Gamma_a^{ML} + \Gamma_c^{ML}) + p_L(\Gamma_a^{L} + \Gamma_c^{L}), \tag{21}$$

$$D_3 = k_{off}(1+F) + p_L(\Gamma_a^{ML} - \Gamma_c^{ML}) + p_{ML}(\Gamma_a^{L} - \Gamma_c^{L}), \tag{22}$$

$$D_4 = p_{ML}(\Gamma_a^{ML} - \Gamma_c^{ML}) + p_L(\Gamma_a^{L} - \Gamma_c^{L}). \tag{23}$$

The coefficients $c_{kl,i}$ determining the signal in experiment II simplify to $c_{43,1} = \frac{1}{2}p_{ML}$, $c_{43,2} = \frac{1}{2}p_L$, $c_{43,3} = -\frac{1}{2}p_{ML}$ and $c_{43,4} = -\frac{1}{2}p_L$. For experiment I all coefficients are positive. The eigenvalues and coefficients determined in the limit of high k_{off} may now be inserted into Eq. (14) to obtain the signal intensities in experiments I and II. We can safely make the assumption that the period over which relaxation occurs satisfies $\tau_m > 1/k_{off}(1+F)$. Since the exponentials involving the larger eigenvalues D_1 and D_3 rapidly drop to zero, the signals are largely determined by the exponentials of the eigenvalues D_2 and D_4. This is equivalent to a unitary transformation of the relaxation matrix that describes the TR-NOESY experiment assuming fast exchange [14–16]. We now obtain the following expressions for the signal amplitudes, which are independent of k_{off}

$$a_{II} \propto \frac{1}{1+F}\sinh[(p_{ML}\Gamma_c^{ML} + p_L\Gamma_c^{L})\tau_m] \times \exp[-(p_{ML}\Gamma_a^{ML} + p_L\Gamma_a^{L})\tau_m], \tag{24}$$

$$a_{I} \propto \frac{1}{1+F}\cosh[(p_{ML}\Gamma_c^{ML} + p_L\Gamma_c^{L})\tau_m] \times \exp[-(p_{ML}\Gamma_a^{ML} + p_L\Gamma_a^{L})\tau_m]. \tag{25}$$

The ratio of the signal intensities in experiments I and II gives the cross-correlated relaxation rate as a population-weighted average of the values for the ligand in the free and bound states

$$\frac{a_{II}}{a_I} = \tanh[(p_{ML}\Gamma_c^{ML} + p_L\Gamma_c^{L})\tau_m]. \tag{26}$$

It is important to note that the requirement for this approximation to hold is that both $[(\Gamma_a^{ML} + \Gamma_c^{ML}) - (\Gamma_a^{L} + \Gamma_c^{L})]/k_{off}$ and $[(\Gamma_a^{ML} - \Gamma_c^{ML}) - (\Gamma_a^{L} - \Gamma_c^{L})]/k_{off}$ must be small. Since the dominant term involves relaxation rates in the bound state, and since the cross-correlation rates can have positive or negative values, the condition may be stated as

$$\frac{\Gamma_a^{ML} + |\Gamma_c^{ML}|}{k_{off}} \ll 1. \tag{27}$$

Ideally, chemical exchange transfer effects are most readily analyzed when this fast exchange condition is satisfied [3]. In TR-NOESY, Γ_a^{ML} and Γ_c^{ML} corresponds to the longitudinal relaxation rates ($1/T_1$) and the cross-relaxation rate, respectively, whereas in TR-CCSY, they

correspond to the transverse relaxation rate ($1/T_2$) and the cross-correlation rate, respectively. The transverse relaxation rates involving multiple quantum coherences increase with the size of the macromolecule and are larger than the longitudinal relaxation rates that affect NOESY. This implies that the condition of fast exchange required for observing exchange transferred cross-correlation can be more difficult to achieve. For example if the bound state has a correlation time τ_c of about 20 ns, and $1/T_2$ of about 86 s^{-1}, exchange rates k_{off} of several 100 s^{-1} might be required for Eqs. (24) and (25) to be valid. Even if the fast exchange condition is fulfilled for observing transferred NOESY effects, the exchange rates might be too slow for observing transferred cross-correlation effects.

4. Mannose–concanavalin A exchange equilibrium

In the following, we examine the binding of mannose to the protein concanavalin A. Of the two anomeric forms of mannose, concanavalin A has a greater affinity for binding the α-anomer. At a pH above 5.6 concanavalin A exists as a tetramer of molecular weight 104 kDa. At a temperature of 303 K, we calculate the approximate isotropic rotational correlation time of the tetramer to be $\tau_c = 39$ ns using the Stokes–Einstein equation [18]. Assuming that the conformations of the two anomers in the bound state are the same as those determined by X-ray diffraction for the pure monosaccharides [19], the approximate spin–lattice relaxation rates for the anomeric proton in the complex ML are expected to be about $1/T_1 = 13\,s^{-1}$ and $52\,s^{-1}$ for the α and β forms, assuming that dipole–dipole relaxation is predominant. This implies that large k_{off}-rates are required to satisfy the fast exchange limit for TR-NOESY where signal intensities become independent of k_{off}. It is therefore necessary to optimise the sample conditions to achieve the fast exchange regime. This is demonstrated in Fig. 1 which shows the H^1–H^2 cross-peak obtained in TR-NOESY experiments at different temperatures. At lower temperatures, the relaxation rate is large while the exchange rate is slow so that the system is far from the fast exchange limit. The cross-peaks are negative with respect to the diagonal peak as expected for the free ligand, which is characterized by a short correlation time. With increasing temperature, the relaxation rate decreases due to faster molecular motion. The exchange rate k_{off}, on the other hand, increases, thus approaching the fast exchange limit. One therefore observes positive cross-peaks of increasing intensity as expected for a bound ligand characterized by the long correlation time τ_c of the complex ML. The fast exchange regime is approached more easily for the α-anomer since its relaxation rate $1/T_1$ in the bound form is about four times slower than the β form. Yet even though the relaxation rate is higher in the β form, its higher k_{off} rate allows exchange transfer effects to be observed in both β and α anomers in a limited temperature range.

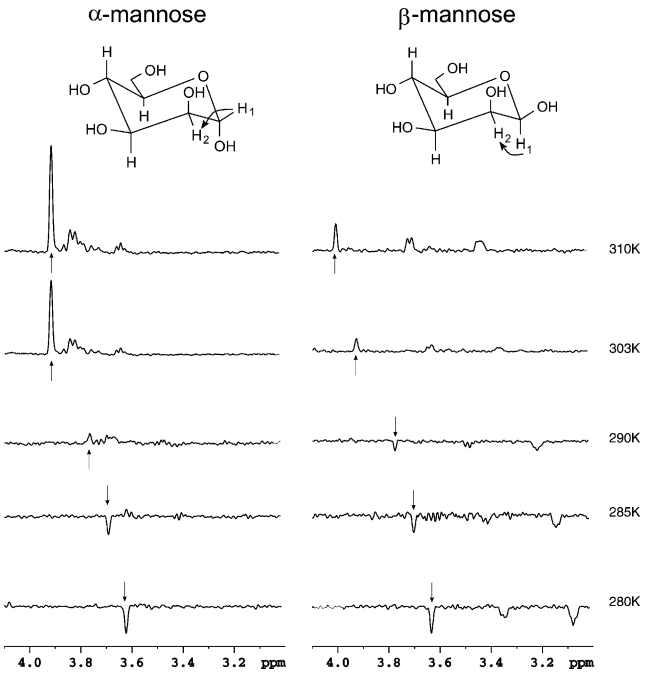

Fig. 1. One-dimensional cross-sections from TR-NOESY spectra showing the H^1-H^2 cross-peaks of α- and β-mannose in the presence of concanavalin A obtained at different temperatures. The sections are taken at the frequency of the H^1 protons in the ω_1 dimension. The fraction of bound ligand was $F = 0.1$ and the spectra were obtained at 600 MHz with a mixing time $\tau_m = 300$ ms. At 280 K the exchange rates are so slow that only negative NOEs within the free ligands are observed. At 310 K, strong positive NOEs result from rapid exchange transfer between the bound and free forms. Also visible in the spectra are cross-peaks due to magnetisation transfer from H^1 to other protons.

Assuming for simplicity that the effective relaxation matrix can be reduced to a 2×2 subsystem, the amplitude of a cross-peak in a TR-NOESY experiment may be calculated using Eq. (14). The rates Γ_a^{ML}, Γ_a^{L} and Γ_c^{ML}, Γ_c^{L} are the self- and cross-relaxation rates corresponding to longitudinal magnetisation [20]. Figs. 2a and 3a show the simulated signal amplitudes for the H^1–H^2 cross-peak in a TR-NOESY experiment for the α- and β-anomers, respectively. The simulations confirm that cross-peaks should be negative for low values of k_{off}. As k_{off} increases the cross-peaks become positive and their amplitudes level off when the fast exchange condition is fulfilled. In Figs. 2b and 3b, we examine the build-up behaviour for various values of k_{off} calculated using Eq. (14). For large k_{off} values, the curves approach the build-up behaviour calculated for the fast exchange limit using Eq. (24), shown by a solid line. The fast exchange limit is approached at lower temperatures for the α-anomer, which is consistent with experimental observations. However, the same conditions did not fulfill the requirements for observing transferred dipole–dipole

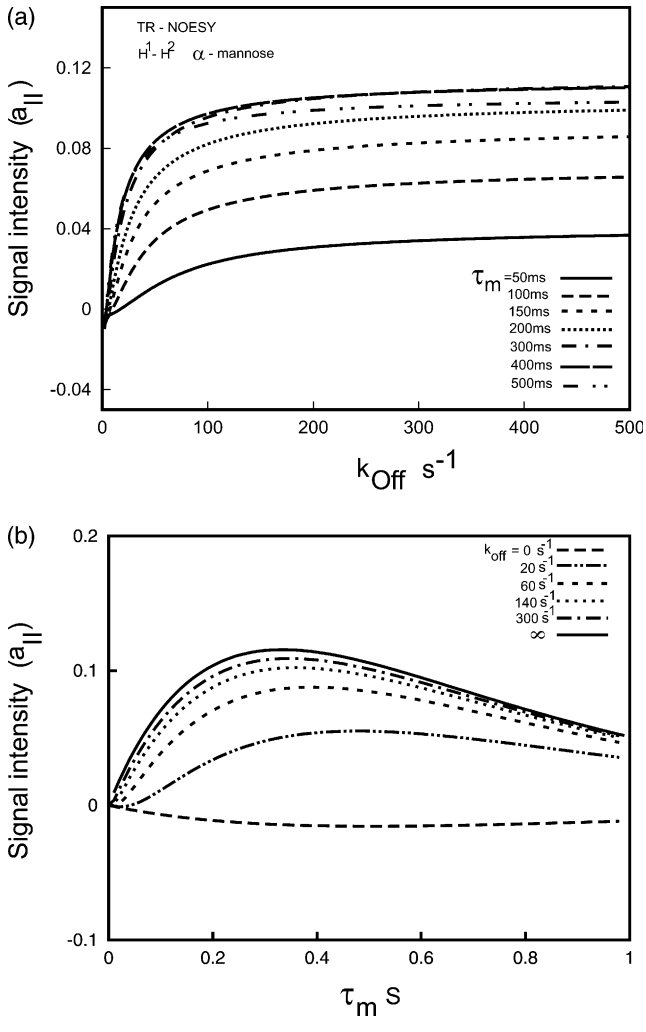

Fig. 2. (a) Simulations of the H^1–H^2 cross-peak signal amplitude a_{II} of α-mannose in a TR-NOESY experiment as a function of the rate k_{off} assuming that the conformation in the bound form is the same as the structure determined by X-ray diffraction in pure α-mannose. The curves correspond to different values of the mixing time τ_m with $F = p_{ML}/p_L = 0.111$. (b) Simulation of the build-up of the H^1–H^2 cross-peak signal amplitude a_{II} for different values of k_{off}. The solid line shows the build-up expected in the fast exchange limit calculated using Eq. (24).

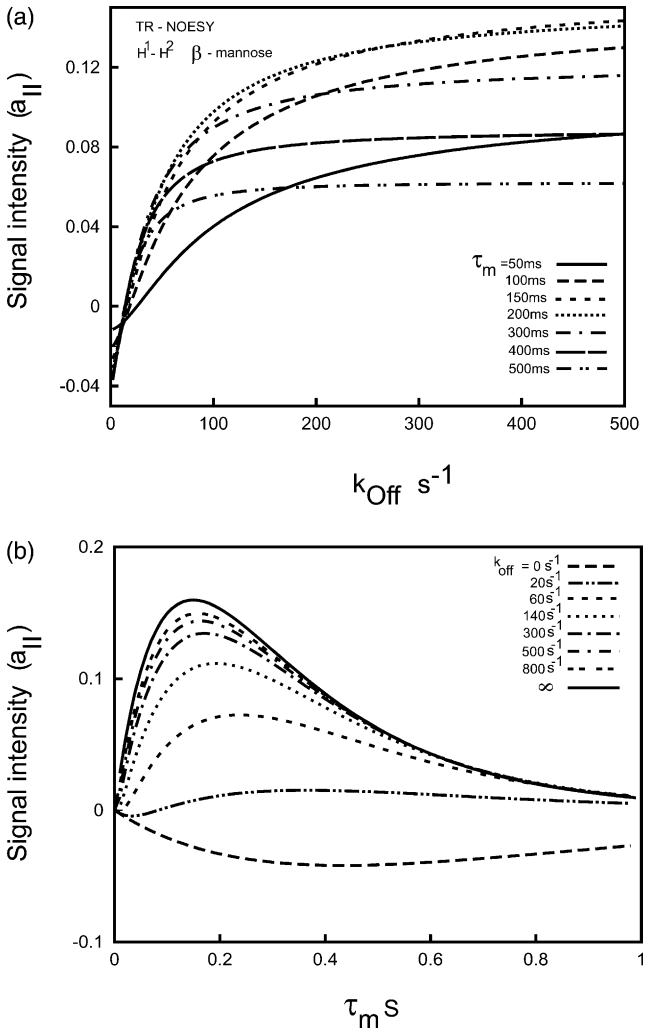

Fig. 3. Simulations of the cross-peak signal amplitude a_{II} in a TR-NOESY experiment similar to Fig. 2 but for the β-anomer.

cross-correlated relaxation effects from the bound to the free state [3]. Indeed it appears that the transverse relaxation rates of the ^{13}C double quantum coherences $4C_{kx}H_{kz}C_{lx}$ and $4C_{ky}C_{ly}H_{lz}$ are too rapid (probably by a factor of 4 or so) compared with the relatively slow k_{off} rate, so that the build-up due to cross-correlation effects in the complex ML could not be monitored successfully by observing the resonances of the free ligand L. Further plans for experimental work will be described after the following discussion of simulations.

We have carried out simulations employing the general expressions for the eigenvalues and coefficients in Eq. (14), to determine the effect of the exchange rate k_{off} on the signal amplitudes in the TR-CCSY experiment. The self-relaxation rates Γ_a^{ML}, Γ_a^{L} and the cross-correlation rates Γ_c^{ML}, Γ_c^{L} were calculated for a H_i–C_j–C_k–H_l spin system in α-mannose assuming again that the solid-state structure determined by X-ray diffraction is preserved in the complex. The experiment monitors the relaxation of zero- and double-quantum coherences involving C_j and C_k over a period τ_m [3]. Under the influence of cross-correlations between the pair of dipolar interactions H_i–C_j and H_l–C_k, there is a partial transformation of the initial coherence $4H_{iz}C_{jx}C_{ky}$ into $4C_{jy}C_{kx}H_{lz}$. Since the chemical shift anisotropy of the sugar carbons are small, we only need to consider the dipolar interactions in the calculations. The self-relaxation rate is given by

$$\begin{aligned}\Gamma_a = {} & (2/3)\{J_{ij}(0) + J_{jl}(0) + J_{ik}(0) + J_{kl}(0)\} \\ & + (1/2)\{J_{jk}(\omega_j) + J_{jk}(\omega_k) + J_{il}(\omega_i) + J_{il}(\omega_l)\} \\ & + \rho_{ij} + \rho_{jl} + \rho_{ik} + \rho_{kl} + \Gamma_1(i) + \Gamma_1(l), \end{aligned} \quad (28)$$

where $\Gamma_1(i)$ and $\Gamma_1(l)$ are the spin–lattice relaxation rates of the protons and,

$$\rho_{ab} = (1/6)J_{ab}(\omega_a - \omega_b) + (1/2)J_{ab}(\omega_a) + (1/2)J_{ab}(\omega_b) + J_{ab}(\omega_a + \omega_b). \quad (29)$$

The spectral density functions J are considered for isotropic rotation [5]. Only the spectral densities at zero frequency are significant in the relaxation rates of the bound form. The dipolar cross-correlated relaxation rate that is responsible for the interconversion of $4H_{iz}C_{jx}C_{ky}$ into $4C_{jy}C_{kx}H_{lz}$ is given by

$$\Gamma_c = (4/3)\{J_{ij,kl}(0) + J_{ik,jl}(0)\}. \quad (30)$$

The second term may be neglected since it involves dipolar interactions over larger distances between non-bonded *C–H* pairs. The correlation time of the free form was assumed to be 0.1 ns. The structural parameters corresponding to the X-ray geometry have been employed in the calculations [19]. The signal amplitudes a_{II} in experiment II correspond to the coherence transfer resulting from the cross-correlations between C^1–H^1 and C^2–H^2 dipolar interactions. The fraction of bound ligand and the duration of the relaxation period were varied to determine their effect on the signal intensities. Fig. 4a shows the expected dependence of a_{II} on k_{off} in α-mannose for different relaxation periods. As k_{off} increases, the cross-peak signal amplitude becomes independent of the exchange rate and approaches the fast exchange limit (Eq. (24)). Two distinct regions are clear from the figure. At low values of k_{off}, the signal amplitude increases on increasing the duration of the relaxation period τ_m. This can be compared to the variation of a_{II} as a function of τ_m expected for a free ligand, $k_{off} = 0$ (Fig. 4b). This implies that in the low k_{off} regime there is no transfer of information from the bound state to the free state through chemical exchange. However as k_{off} increases, there is a build-up of the signal resulting from coherence transfer as is clear from Fig. 4b. The build-up of a_{II} as a function of τ_m calculated from Eq. (24) under fast exchange conditions is shown in Fig. 4b. Comparison with the simulations in Fig. 2 show that even for k_{off} values which show significant TR-NOESY effects, the curves for TR-CCSY can still be in the regime where transfer effects cannot be observed.

In Fig. 5a we examine the influence of the ratio F of the bound to free ligand. Again the fast exchange behaviour is visible on the right-hand side, where the dependence on F may be compared with the results from Eq. (24) shown in Fig. 5b. A similar increase followed by a decay with increasing fraction of the bound form is also observed in transferred NOESY in the fast exchange regime [20]. The simulations clearly show that large k_{off}-rates are required to fulfill the requirements of the fast exchange regime [where Eqs. (24) and (25) are valid] on the time scale of the relaxation rates of multiple quantum coherences. Except for very weakly

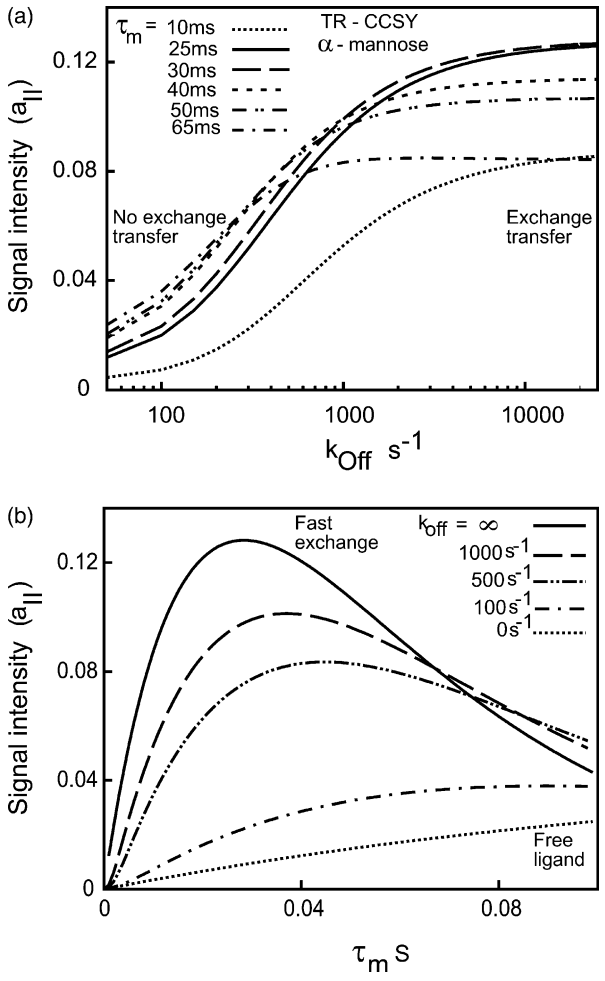

Fig. 4. (a) Simulations of the signal amplitude a_{II} in an exchange transferred cross-correlation (TR-CCSY) experiment as a function of k_{off} for different durations of the relaxation interval τ_m for the H^1–C^1–C^2– H^2 unit in α-mannose. (b) Comparison of the dependence of the signal amplitude a_{II} on the duration of the relaxation period τ_m for an equilibrium in fast exchange (using Eq. (24)) and for a free ligand. Curves for some intermediate values of k_{off} obtained using Eq. (14) are also included. All calculations were carried out for $F = 0.111$.

binding ligands, it is preferable to have bound states with relatively short correlation times τ_c^{ML} for observing exchange-transferred cross-correlation effects. In Fig. 6 we examine the effect of different bound state correlation times. As the correlation times decrease, the fast exchange regime shifts to lower k_{off} values. Fig. 7 shows simulations carried out for different *H–C–C–H* units in α-mannose corresponding to different dihedral angles. The fast exchange regime is attained at the lowest k_{off} for the case where the sum of the self-relaxation rate and the absolute value of the cross-correlated relaxation rate (see Eq. (27)) is the lowest.

Further experimental work is in progress to reduce the correlation time of τ_c^{ML} of the complex ML (a succinylated derivative of concanavalin A is known to form dimers rather than tetramers, which should

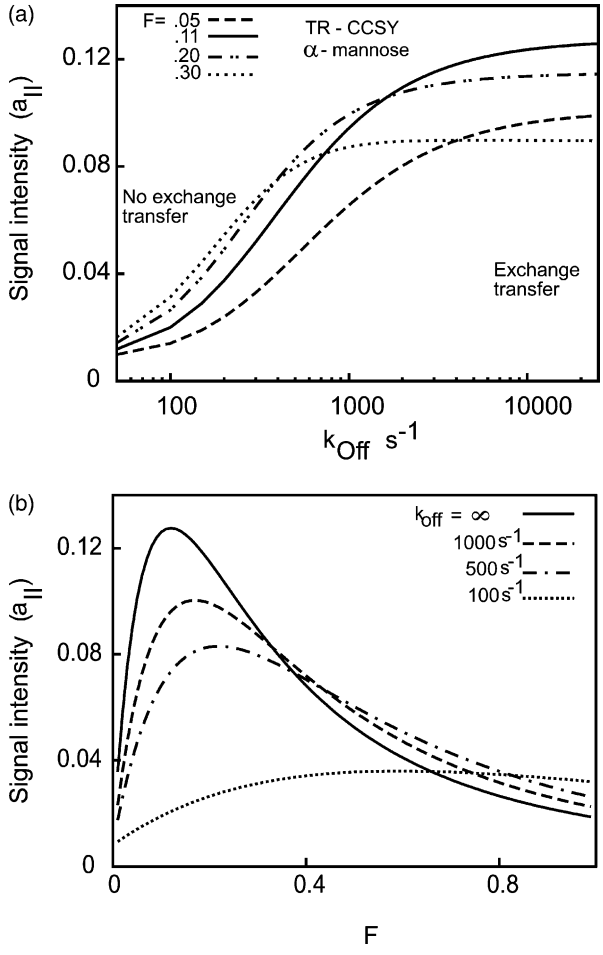

Fig. 5. (a) Simulations of the signal amplitude a_{II} in a TR-CCSY experiment as a function of k_{off} for different ratios $F = p_{ML}/p_L$ for the H^1–C^1-C^2- H^2 unit in α mannose. (b) Dependence of the signal amplitude a_{II} on the ratio F for an equilibrium in fast exchange calculated for $\tau_m = 0.25$ ms using Eq. (24). Curves for some intermediate values of k_{off} obtained using Eq. (14) are also included.

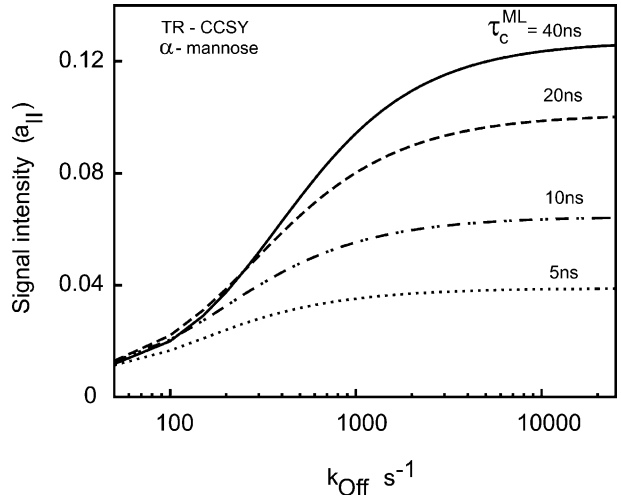

Fig. 6. Calculated signal amplitude a_{II} for the H^1–C^1-C^2– H^2 unit of α-mannose in a TR-CCSY experiment as a function of k_{off} for different correlation times of the bound form ($\tau_m = 0.25$ ms, $F = 0.111$).

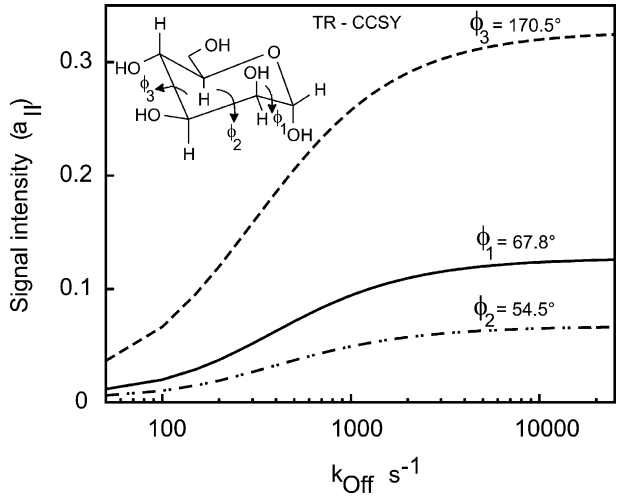

Fig. 7. Calculated signal amplitude a_{II} in a TR-CCSY experiment as a function of k_{off} expected for various *HCCH* four spin subsystems in α-mannose with different dihedral angles assuming the structure determined by X-ray diffraction. The curves correspond to dipolar cross-correlations between C^1–H^1 and C^2–H^2 (dihedral angle $\phi_1 = 67.8°$), C^2–H^2 and C^3-H^3 (dihedral angle $\phi_2 = 54.5°$), C^3–H^3 and C^4–H^4 (dihedral angle $\phi_3 = 170.5°$). Calculations are for $\tau_c = 38.7$ ns, $\tau_m = 0.25$ ms and $F = 0.111$.

diminish τ_c^{ML} by a factor two) and to avoid paramagnetic contributions to the relaxation of the carbon-13 double quantum coherences (it is possible to replace the Mn^{2+} ions of natural concanavalin A by Zn^{2+} ions, apparently without affecting its protein fold or its affinity for mannose.) We also plan to investigate TR-CCSY of glucose, which has a weaker affinity for concanavalin A than mannose, and presumably a larger k_{off}-rate. Following a suggestion by Griesinger (private communication), we shall also explore if the expectation values of the carbon-13 double quantum coherences can be temporarily 'stored' in the form of longitudnal three-spin order terms such as $4C_{kx}H_{kz}C_{lx}$ and $4C_{ky}C_{ly}H_{lz}$, which should be less prone to relaxation and more amenable to be transferred to the free ligand L even if the k_{off} rate is relatively slow.

5. Conclusions

Simulations of signal amplitudes in TR-NOESY and TR-CCSY based on analytical expressions have been carried out for fast, intermediate and slow chemical exchange. The signal intensities have been examined as a function of the mixing time τ_m, the correlation time τ_c of the complex, the lifetime $\tau_{ex} = 1/k_{off}$ of the complex, and the fraction F of the bound ligand. Exchange transfer experiments for obtaining bound state structure are most suitable when the condition of Eq. (27) is satisfied. Ideally, this requires small relaxation rates in the bound state and high exchange rates which can be controlled to some extent by a suitable choice of

experimental conditions such as temperature, pH, salt concentration etc. The mixing time τ_m and the fraction of the bound ligand F may be optimized for maximizing the signal intensity in experiment II. In general, for larger macromolecules, shorter mixing times and smaller fractions of bound ligand lead to maximum signal. Most importantly, we conclude that observing a TR-NOESY effect does not necessarily imply that the exchange rates also permit the observation of a TR-CCSY effect involving multiple quantum coherences. This is particularly true in the case of ligands binding to large macromolecules. In situations where both TR-NOESY and TR-CCSY effects can be observed, it is possible that while the fast exchange condition is satisfied for the former, the latter could still be in an intermediate exchange regime. This means that the interpretation of signal amplitude ratios obtained from experiments I and II in terms of a population weighted average of cross-correlated relaxation rates [Eqs. (24) and (25)] would not be strictly correct in such cases. A correct analysis of such experiments should not only yield information on the conformation of bound ligands, but also on the k_{off}-rates of the dissociation of the complexes which are difficult to determine otherwise.

Acknowledgments

This work was supported by the Centre National de la Recherche Scientifique (CNRS) of France, and by the Fonds National de la Recherche Scientifique (FNRS) and the Commission pour la Technologie et l'Innovation (CTI) of Switzerland.

References

[1] P. Balram, A.A. Bothner-By, J. Dadok, Negative nuclear Overhauser effects as probes of macromolecular structure, J. Am. Chem. Soc. 94 (1972) 4015–4017.

[2] Y. Lian, I.L. Barsukov, M.J. Sutcliff, K.H. Sze, G.C.K. Roberts, Protein–ligand interactions: exchange processes and determination of ligand conformation and protein–ligand contacts, Methods Enzymol. 239 (1994) 657–700.

[3] T. Carlomagno, I. Felli, M. Czech, R. Fischer, M. Sprinzl, C. Griesinger, Transferred cross-correlated relaxation: application to the determination of sugar pucker in an aminoacylated tRNA-mimetic weakly bound to EF-Tu, J. Am. Chem. Soc. 121 (1999) 1945–1948.

[4] M.J.J. Blommers, W. Stark, C.E. Jones, D. Head, C.E. Owen, W. Jahnke, Transferred cross-correlated relaxation complements transferred NOE: structure of an IL-4R-derived peptide bound to STAT-6, J. Am. Chem. Soc. 121 (1999) 1949–1953.

[5] A. Kumar, R.C.R. Grace, P.K. Madhu, Cross-correlations in NMR, Prog. Nucl. Magn. Reson. Spectrosc. 37 (2000) 191–319.

[6] B. Brutscher, Principles and applications of cross-correlated relaxation in biomolecules, Concepts Magn. Reson. 12 (2000) 207–229.

[7] E. Chiarparin, P. Pelupessy, R. Ghose, G. Bodenhausen, Relaxation of two-spin coherence due to cross-correlated fluctuations of dipole–dipole couplings and anisotropic shifts in NMR of ^{15}N,^{13}C-labeled biomolecules, J. Am. Chem. Soc. 121 (1999) 6876–6883.

[8] B. Reif, A. Diener, M. Hennig, M. Maurer, C. Griesinger, Cross-correlated relaxation for the measurement of angles between tensorial interactions, J. Magn. Reson. 143 (2000) 45–68.

[9] B. Reif, M. Hennig, C. Griesinger, Direct measurement of angles between bond vectors in high-resolution NMR, Science 276 (1997) 1230.

[10] D. Yang, R. Konrat, L.E. Kay, A multidimensional NMR experiment for measurement of the protein dihedral angle based on cross-correlated relaxation between $^1H^\alpha$–$^{13}C^\alpha$ dipolar and $^{13}C'$ (carbonyl) chemical shift anisotropy mechanisms, J. Am. Chem. Soc. 119 (1997) 11938–11940.

[11] I. Felli, C. Ritcher, C. Griesinger, H. Schwalbe, Determination of RNA sugar pucker mode from cross-correlated relaxation in solution NMR spectroscopy, J. Am. Chem. Soc. 121 (1999) 1956–1957.

[12] J. Boisbouvier, B. Brutscher, A. Pardi, D. Marion, J.P. Simorre, NMR determination of sugar puckers in nucleic acids from CSA-dipolar cross-correlated relaxation, J. Am. Chem. Soc. 122 (2000) 6779–6780.

[13] C. Zwahlen, S.J.F. Vincent, L. Di Bari, M.H. Levitt, G. Bodenhausen, Quenching spin diffusion in selective measurements of transient Overhauser effects in nuclear magnetic resonance. Applications to oligonucleotides, J. Am. Chem. Soc. 116 (1994) 362–368.

[14] S.B. Landy, B.D.N. Rao, Dynamical NOE in multiple-spin systems undergoing chemical exchange, J. Magn. Reson. 81 (1989) 371–377.

[15] F. Ni, Complete relaxation matrix analysis of transferred nuclear Overhauser effects, J. Magn. Reson. 96 (1992) 651–656.

[16] R.E. London, M.E. Perlman, D.G. Davis, Relaxation-matrix analysis of the trasnferred nuclear Overhauser effect for finite exchange rates, J. Magn. Reson. 97 (1992) 79–98.

[17] W. Lee, N. Ramakrishna, Influence of conformational exchange on the 2D NOESY spectra of biomolecules existing in multiple conformations, J. Magn. Reson. 98 (1992) 36–48.

[18] R.T. Boeré, R.G. Kidd, Rotational correlation times in nuclear magnetic relaxation, Annu. Rep. NMR Spectrosc. 13 (1982) 320–385.

[19] P.F. Longchambon, D. Avenel, A. Neuman, Structure cristalline de l'alpha-D-mannopyrannose, Acta Cryst. B32 (1976) 1822.

[20] P.A. Campbell, B.D. Sykes, Theoretical evaluation of the two-dimensional transferred nuclear Overhauser effect, J. Magn. Reson. 93 (1991) 77–92.